

STUDY OF THE INFLUENCE OF MAGNETIC FIELD PROFILE ON PLASMA PARAMETERS IN A SIMPLE MIRROR TRAP

M. Mazzaglia^{1,†}, G. Castro¹, D. Mascali¹, R. Miracoli³, S. Briefi², U. Fantz², L. Celona¹, E. Naselli^{1,4}, R. Reitano^{1,4}, G. Torrìsi¹ and S. Gammino¹

¹ INFN – Laboratori Nazionali del Sud, Catania, Italy

² Max-Planck-Institut für Plasmaphysik, Garching, Germany

³ ESS Bilbao, Zamudio, Spain

⁴ Università degli studi di Catania, Catania, Italy

Abstract

This work presents the multiple diagnostics characterization of the plasma in an axis-symmetric simple mirror trap as a function of magnetic field profile (mirror ratios and magnetic field gradient), especially in the quasi-flat B field configuration that is typical of Microwave Discharge Ion Sources, and also of neutral gas pressure and microwave power. The simultaneous use of Optical Emission Spectroscopy, Langmuir Probe and X-ray diagnostics allows the characterization of the whole electron energy distribution function (EEDF), from a few eV to hundreds of keV. Results show non-linear behaviour under small variations of even one source parameter and strong influence on EEDF of the B_{\min}/B_{ECR} ratio. Benefit and next developments will be highlighted.

INTRODUCTION

Plasma diagnostics plays a crucial role for the development of high-performance ion sources for accelerators. A detailed knowledge of the electron energy distribution function (EEDF) is mandatory for any improvement of existing or future devices. For sake of compactness (mechanical constraints limit ECRIS ion source accessibility), historically only a limited number of diagnostics have been applied to ECRIS plasmas. Therefore, in most of the cases, plasma properties were only estimated from semi-empirical considerations. Over the last years, few groups have directly probed ECRIS plasma via diagnostics [1, 2, 3, 4]. Never performed in the past, multi-diagnostics allow to measure simultaneously plasma parameters in different energy domains. At LNS we plan to implement a multi-diagnostics system able to probe the plasma from RF to gamma-ray emission, performing space and time-resolved measurements. In this paper we present data already acquired in multi-diagnostics, at the Flexible Plasma Trap (FPT) test-bench [5], using at the same time Langmuir Probe (LP), optical Emission Spectroscopy (OES) and X-Ray spectroscopy. Despite the results have been obtained on a test-bench, the plasma trap emulates several features of existing ECRIS, and especially we hereby will focus the

simple-mirror and Flat-B field configurations which is common in the field of Microwave Discharge Ion Sources for high current proton beams. The simultaneous use of these different diagnostics allowed to characterize the plasma parameters as a function of the applied external magnetic field, of microwave power and gas pressure.

EXPERIMENTAL SETUP AND DIAGNOSTIC METHODS

Multi-diagnostics measurements have been carried out on the FPT, installed at INFN-LNS and described in [5]. Figure 1 shows a schematic diagram of the FPT, including the RF power injection system, the three magnetic coils, LP, OES and X-rays diagnostics.

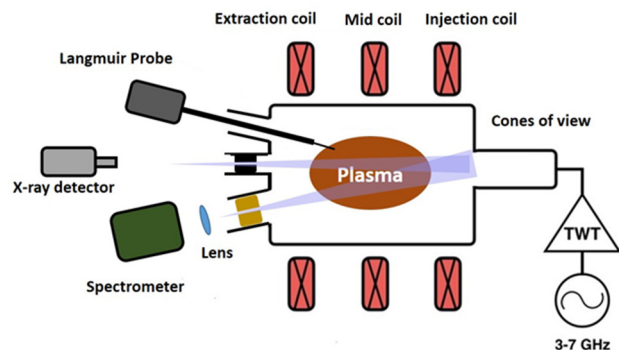


Figure 1: Schematic of the FPT experimental setup at the INFN-LNS.

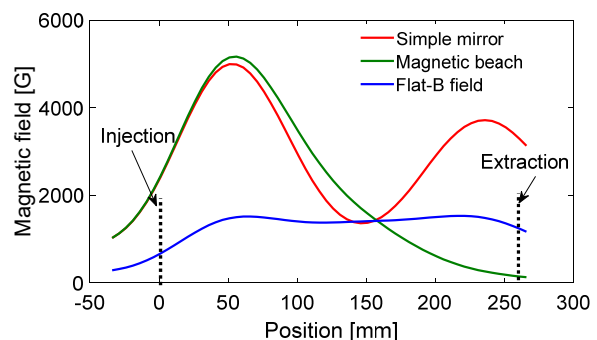


Figure 2: Magnetic field profiles that can be generated by the FPT.

† maria.mazzaglia@lns.infn.it

The solenoids have been developed in order to allow the generation of different magnetic configurations, from flat-B field to simple mirror or magnetic beach (see Fig. 2).

In this work, we investigated the plasma generated in flat-B field configuration. Microwaves have been generated by a Travelling Wave Tube (TWT) operating in the range 4-7 GHz. Hereinafter, a brief introduction to the diagnostics used during the experimental campaign is given.

LP diagnostics: The Langmuir Probe (LP), although is an invasive diagnostic, represents the easiest way to perform the measurements of density and temperature of low energy plasma electrons (1-100 eV). The probe consists of a tungsten tip with a diameter of 125 μm and a length of 4 mm, inserted in a tungsten core coated with alumina. The plasma parameters have been obtained by the resistivity curve using the theoretical model described in [6]. LP data have been used as cross-checks and benchmarks of OES measurements.

OES diagnostics: OES provide a method to determine plasma parameters in a non-invasive way. However, these diagnostics have the drawback that only line-of-sight-integrated results are obtained. Spectroscopic measurements have been carried out with an intensity-calibrated survey spectrometer ($\Delta\lambda_{\text{FWHM}} \approx 1 \text{ nm}$) for the Balmer series of atomic hydrogen (H_α to H_γ) as well as for the Fulcher- α transition of the H_2 molecule ($d^3\Pi_u \rightarrow a^3\Sigma_u^+$). The measured emissivities have been evaluated with the collisional radiative (CR) models Yacora H and Yacora H_2 [7]. The plasma parameters have been estimated by comparing the line ratio measured during the experimental campaign with the theoretical line ratio estimated by means of a CR model. In particular, we used the H_β/H_γ and H_α/H_β ratios to determine electron density and temperature and $H_\gamma/H_{\text{Fulch}}$ ratio to determine the relative abundance between atomic and molecular hydrogen n_H/n_{H_2} .

X-ray diagnostics: The X-ray volumetric measurement is a powerful method for determining density and temperature of medium-high energy plasma electrons ($> 1 \text{ keV}$). The X-ray flux requires a proper collimation for fixing the solid angle covered by the X-ray detector and an adequate emissivity model for the data evaluation. The plasma emissivity model used is described in references [3, 8]. The X-ray measurements have been carried out with two different detectors: High Purity Germanium (HpGe) for the detection of X-rays in the range 1-100 keV and Silicon Drift Detector (SDD) able to reveal X radiation in the range 1-30 keV.

EXPERIMENTAL RESULTS

The experimental campaign has been carried out in different conditions of neutral pressure, microwave power and magnetic field profile. FPT is a very versatile machine which can operate in Simple Mirror with the possibility to tune the trap at different mirror ratios. That is of particular importance for studying the ECR heating processes as a

function of the magnetic field structure and, in particular, to explore the plasma instabilities triggered by the B-field itself. For this reason, most of the experimental campaign has been devoted to simple-mirror operations, and a wide analysis of the collected data is going to be published elsewhere [9]. For sake of brevity we hereby present a short summary of what obtained in simple-mirror, and a wider analysis of flat-B field configuration. In simple-mirror configuration the microwave frequency has been set at 6.83 GHz. The change in mid coil current allowed to modify the $B_{\text{min}}/B_{\text{ECR}}$ ratio along the chamber axis from 0.56 to 1.04. The measurements have been carried out at two different pressures ($1.5 \cdot 10^{-4}$ and $2 \cdot 10^{-3}$ mbar) and microwave power fixed at 30 and 80 W. While, in flat-B field configuration, the microwave frequency has been set at 4.13 GHz, microwave power at 80, 130 and 160 W and pressure at $1.5 \cdot 10^{-4}$ mbar.

We present data from both the magnetic configurations only from LP data. Electron density and temperature versus the position at $2 \cdot 10^{-3}$ mbar, in simple mirror configuration, are respectively shown in Figs. 3 and 4.

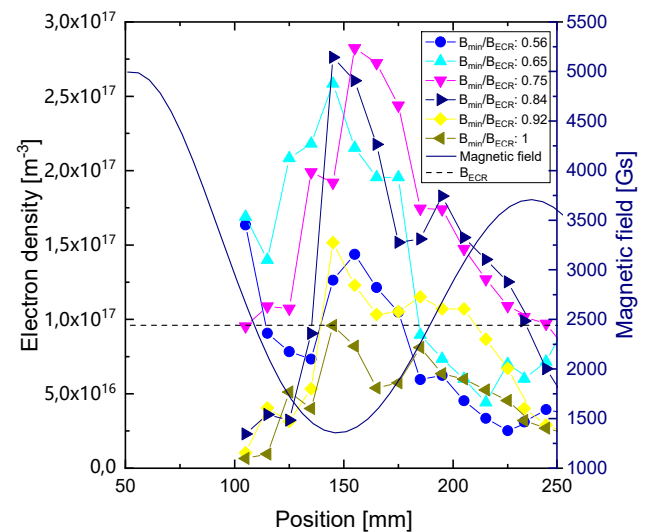


Figure 3: Electron density profiles evaluated by means of LP at 80 W microwave power and $2 \cdot 10^{-3}$ mbar pressure.

Maximum average and peak density is obtained when $0.65 < B_{\text{min}}/B_{\text{ECR}} < 0.84$. The plasma density then drops and at $B_{\text{min}}/B_{\text{ECR}}$ approaching the unity it collapses of a factor five. For smaller ratios the plasma is well peaked around the midplane of the plasma chamber, due to the effective magnetic trapping. Then, the density distribution flattens due the weaker and weaker trapping efficiency.

Concerning the electron temperature (LP is able to probe only the so-called “cold” population), it lies in the range 4-14 eV and it reaches the maximum values around the ECR layers.

Figures 5 and 6 respectively show electron density and temperature versus position at $1.5 \cdot 10^{-4}$ mbar, in flat-B field configuration.

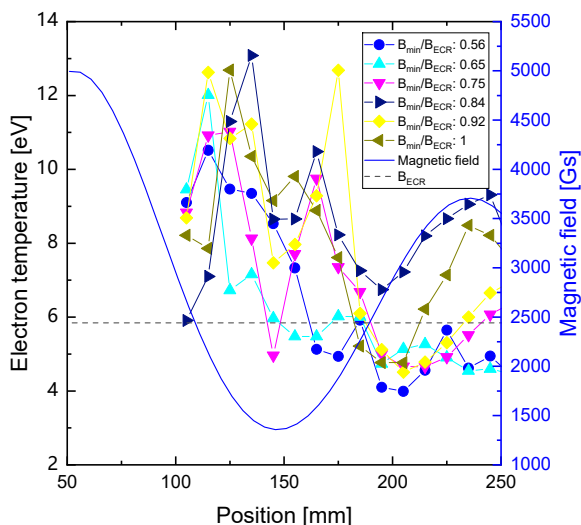


Figure 4: Temperature profiles evaluated by means of LP for 80 W microwave power and $2 \cdot 10^{-3}$ mbar pressure.

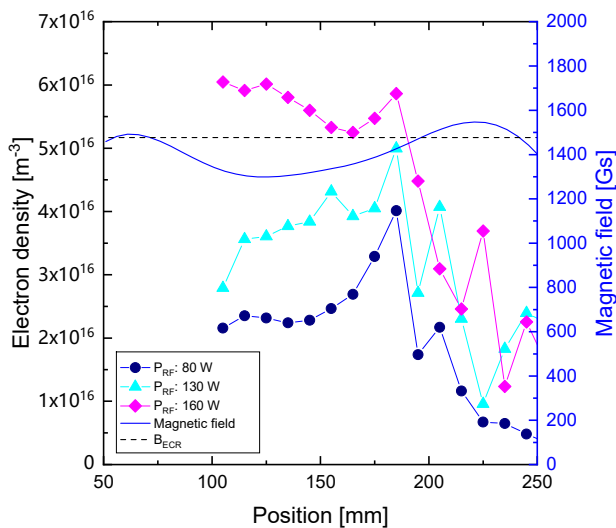


Figure 5: Electron density profiles evaluated by means of LP for three microwave power value (80, 130 and 160 W) and $1.5 \cdot 10^{-4}$ mbar pressure.

It is interesting to compare simple mirror and flat-B configurations. First of all, the absolute value of the plasma density is a factor five lower in flat-B with respect to the simple mirror case. The data comparison shows that the other main difference – as expected – consists in the different distribution of the plasma in the chamber. Simple mirror configuration is acting as a trap for the electrons so that the plasma density is peaked in the central part. However, the comparison with other diagnostics say that the magnetic profile is acting also on the phase space, i.e. on the plasma heating process. X-ray flux dramatically increases when increasing the B_{min} (see data commented in [9, 10]), up to 10^4 cps. A different situation occurs for flat-B field measurements. Only a slight trapping is evident and a much lower X-ray rate was detected (in particular, around

10^2 cps for the lowest pressure regime, i.e. a factor 100 lower than for the simple-mirror configuration) at least in the RF power range we could explore.

In terms of plasma density, LP data in flat-B field configuration were collected for different RF power, showing a clear increase of the plasma density and a broader and broader distribution of the plasma in the chamber (that means a larger number of electrons and ions is generated).

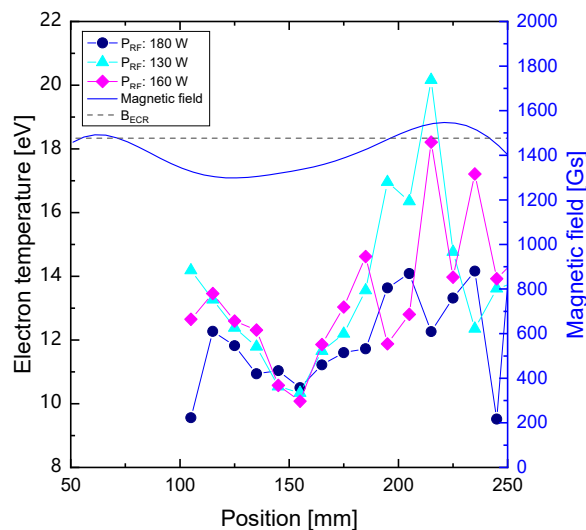


Figure 6: Electron temperature profiles evaluated by means of LP for three microwave power value (80, 130 and 160 W) and $1.5 \cdot 10^{-4}$ mbar pressure.

Concerning the electron temperature, Fig. 6 shows that on average T_e lies in the range 10-20 eV, with some clear peaks (the same for more or less all the RF power levels) occurring close to the ECR layers.

Figure 7 shows the results of the electron density and temperature versus pressure.

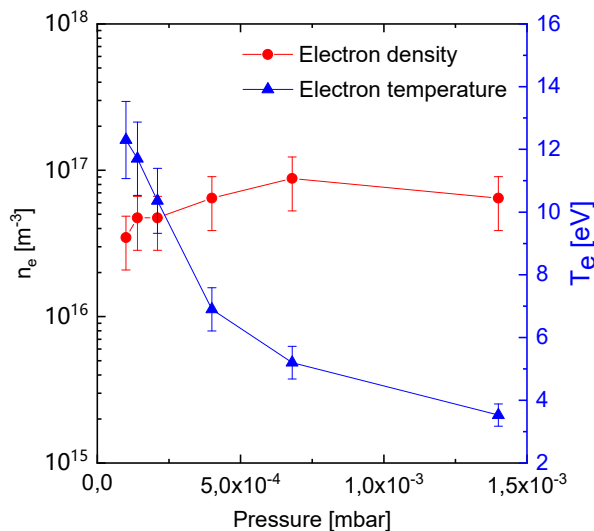


Figure 7: Electron density and temperature obtained from the OES evaluations for varying pressure.

Content from this work may be used under the terms of the CC BY 3.0 licence (© 2018). Any distribution of this work must maintain attribution to the author(s), title of the work, publisher, and DOI.

Electron density slightly increases with pressure from $\approx 3 \cdot 10^{16}$ to $\approx 8 \cdot 10^{16} \text{ m}^{-3}$, whereas the electron temperature decreases from about 12 to 4 eV. Finally, Fig. 8 shows the density ratio of atomic to molecular hydrogen versus pressure. $n(\text{H})/n(\text{H}_2)$ ratio decreases as pressure increases, which can be explained arguing that the continuous injection of H_2 molecules is not compensated by molecules breakdown due to the constant microwave power.

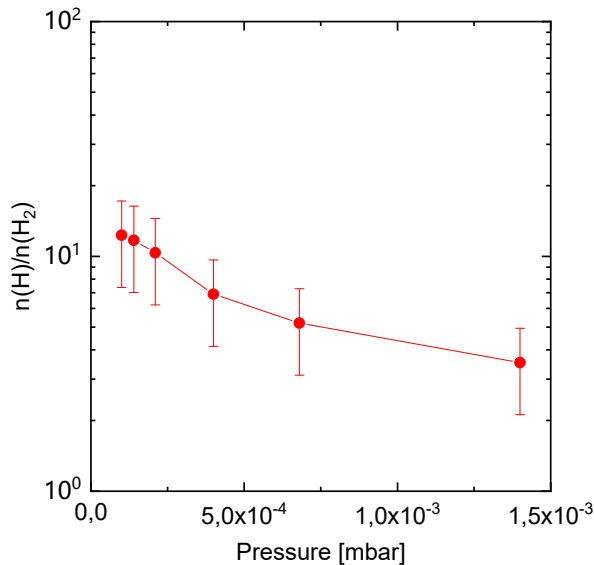


Figure 8: Density ratio of atomic to molecular hydrogen obtained from the OES evaluations for varying pressure.

OES estimations of density and temperature agree very well with the LP data, more than in case of simple-mirror configuration. This may be due to the fact that OES only provide line-of-sight averages of these observables, that in simple mirror configuration are heavily affected by gradients and non-homogeneities of the plasma. In flat-B field, instead, the temperature and density distribution appear to be much smoother.

CONCLUSION AND PERSPECTIVES

The paper reports about an experimental campaign performed with a versatile machine which is able to emulate important features of plasma based ion sources: the axial trapping due to simple-mirror magnetic configuration, or the flat-B field configuration typically used in high intensity proton sources. Data have been collected in multi-diagnostics mode, using simultaneously a Langmuir probe and Optical Emission Spectroscopy, as well as soft-X ray detectors. The plasma density and temperature have been measured in terms of different tunings, and especially in terms of the magnetic field profile. About the point, it is worth mentioning the most significant result was the experimental demonstration of the “scaling rules” impact on the plasma density. In the ECRIS community, in fact, it is well known that the optimal performances are obtained

when $B_{\text{min}}/B_{\text{ECR}}$ is around 0.65 or 0.7. Our measurements are perfectly consistent with this semi-empirical rule, since they show that at those ratios the axial confinement is the most efficient in terms of absolute values of the density and production of X-rays. Smaller ratios mean lower electron temperatures (detrimental for stepwise ionization towards highly charge ions), while larger ratios induce to plasma instabilities, as demonstrated by other authors [11].

In perspective, we plan to further improve the setup including space resolved X-ray spectroscopy and higher resolution optical emission spectroscopy.

Measurements on both simple-mirror and flat-B configuration can drive the design of future ECRIS or MDIS, as well as the better tuning of the existing ones.

ACKNOWLEDGEMENTS

The technical support of Salvo Vinciguerra, Salvo Marletta, Antonino Maugeri, Angelo Seminara, is warmly acknowledged.

The activities presented in this paper have been supported by the PANDORA grant, funded by the 5th Nat. Comm. of INFN, and from the European Spallation Source collaboration.

REFERENCES

- [1] R. Kronholm *et al.*, *Rev. sci. instrum.*, vol. 89, p. 043506, (2018).
- [2] N. K. Bibinov *et al.*, *Plasma Sources Sci. Technol.*, vol. 14 (2005).
- [3] D. Mascali *et al.*, *Rev. sci. instrum.*, vol. 85, p. 02A956, (2014).
- [4] R. Rácz *et al.*, *Plasma Sources Sci. Technol.*, vol. 26, p. 075011, (2017).
- [5] S. Gammino *et al.*, *Rev. Jurnal Instrum.*, vol. 12 (2017).
- [6] G. Castro *et al.*, *Plasma Sources Sci. Technol.*, vol. 26, p. 055019, (2017).
- [7] D. Wunderlich and U. Fantz, *Atoms*, vol. 4 p. 26, (2016).
- [8] D. Mascali *et al.*, *Rev. sci. instrum.* vol. 87, p. 02A510, (2016).
- [9] S. Brieñi *et al.*, submitted to *Plasma Sources Sci. Technol.*
- [10] R. Miracoli *et al.*, *these Proceedings*.
- [11] I. Izotov *et al.*, *Plasma Sources Sci. Technol.* vol. 24, p. 045017, (2015).